

**Key words:**  $\Delta J$ -integral range, fatigue crack growth rate, stress ratio, finite element method

DARIUSZ ROZUMEK \*

## J-INTEGRAL IN THE DESCRIPTION OF ELASTO-PLASTIC CRACK GROWTH KINETICS CURVE

The paper presents kinetic fatigue crack growth curve for 10HNAP steel, which is verified experimentally. An energy approach based on the  $\Delta J$ -integral range is shown. The tests have been carried out on plane specimens with notches under tension-compression for three values of stress ratio  $R$ . The  $J$ -integral is calculated analytically and by the finite element method. A relationship for the description of the whole kinetic crack growth curve including  $J$ -integral is presented. It is shown that at the constant loading and the change of stress ratio  $R$  from  $-1$  to  $0$  the fatigue crack growth rate increases. A relationship is proposed in the paper for description of the kinetic crack growth curve. It gives results that are consistent with experimental ones and those obtained with the use of the finite element method (FEM).

### Nomenclature

$D$	– coefficient in the empirical formula,
$E$	– Young's modulus,
$J_{Ic}$	– critical value of the integral,
$J_{max}$	– maximum $J$ -integral,
$J_{min}$	– minimum $J$ -integral,
$K_{max}$	– maximum stress intensity factor,
$K_{min}$	– minimum stress intensity factor,
$P_a$	– amplitude of load,
$P_m$	– mean load,
$R$	– stress ratio,
$Y$	– correction factor of specimen,
$a$	– half length of the crack,

---

\* *Opole University of Technology, Faculty of Mechanical Engineering, ul. S. Mikotajczyka 5, 45-271 Opole, Poland; E-mail: drozumek@po.opole.pl*

$da/dN$	– fatigue crack growth rate,
$p$	– exponent in the empirical formula,
$\Delta J$	– total J-integral range,
$\Delta J_e$	– elastic component of J-integral range,
$\Delta J_p$	– plastic component of J-integral range,
$\Delta J_{th}$	– threshold J-integral range,
$\Delta K$	– stress intensity factor range,
$\Delta K_{th}$	– threshold stress intensity factor range,
$\Delta \varepsilon$	– strain range,
$\Delta \varepsilon_e$	– elastic strain range,
$\Delta \varepsilon_p$	– plastic strain range,
$\Delta \sigma$	– stress range,
$\nu$	– Poisson's ratio,
$\sigma_y$	– yield stress,
$\sigma_u$	– ultimate stress.

## 1. Introduction

Classical equations of fatigue crack growth kinetics from the threshold value to the critical value characterising fracture toughness are derived on the basis of experimental results obtained at different loadings. Priddle [1] was one of the first investigators who did that. He described crack growth kinetics curve versus stress intensity factor range  $\Delta K$ . Following Priddle's equation, Jarema [2] substituted the intensity factor range  $\Delta K$  by the maximal intensity factor  $K_{max}$ . Another relation for crack growth kinetics curve described by stress intensity factor range, which included stress ratio, was introduced by McEvily [3]. Other relations for the description of the whole sigmoidal curve, which appeared later can be found in the papers [4], [5]. The relations published there are true for the materials in which the plastic zone is small in comparison with the body geometry. In the case of long range plastification, the stress intensity factor or its range should not be used for the estimation of fatigue crack growth rate as these quantities are not the measure of stresses at the crack tip [6]. In the paper [7], the J-integral has been established as a failure criterion for stable or unstable crack growth [8]. Under large scale yielding fatigue crack growth rate can be related to the cyclic  $\Delta J$ -integral range, as originally proposed by Dowling and Begley [9]. However, with an increase in plastic deflection, the fatigue crack growth will also deviate. Dowling and Begley [9] compared the results obtained on the basis of their theoretical relation with experimental results. They observed a good agreement between them in the case of deflection control. However, for tests under load control, there was a significant deviation. They concluded

that the crack growth rates during incremental plastic deflection cannot be predicted by only the  $\Delta J$ -integral range criterion, and a more general criterion that includes the effect of the mean  $\Delta J$  level is needed. Considering this problem, one of the authors [10] described the fatigue crack growth rate versus  $\Delta J$ -integral range for different stress ratios. The tests performed were cyclic bending of specimens for two different kinds of steel under load control. The proposed formula in paper [10] for the description of fatigue crack growth rate, including  $\Delta J$ -integral range, satisfactorily describes the results obtained experimentally. The equation presented in [9] describes the II linear crack range, whereas the empirical formula [10] pertains to the II and III range of the crack kinetics curve, i.e. to the critical value of  $J_{Ic}$  integral. None of the presented energetic approaches includes the threshold value of  $J_{th}$  integral. The complete crack growth kinetics curve versus  $\Delta J$ -integral range was introduced in [11]. As it did not include the mean level, it led to discrepancies between the experimental results and the equation for higher mean stress values.

The experimental relation introduced in the paper describes the crack growth kinetics curve, i.e. from the threshold value range  $\Delta J_{th}$  to the critical value of  $J_{Ic}$  integral. Apart from that, the equation includes the stress ratio  $R$ , which significantly affects the fatigue crack growth rate, as it is shown in [12]. During the tests it has been found that for small strains in the linear-elastic range, the cyclic  $J$ -integral does not depend on loading, as in the case of the monotonic  $J$ -integral. For large strains in the elastic-plastic range, the cyclic  $J$ -integral depends on loading. Analysing the influence of successive loading cycles at the changing plastic zone during a crack growth course one can find that the cyclic  $J$ -integral remains constant during loading (unloading) except for the first monotonic stage of loading. The performed tests confirmed Tanaka's observations [13].

## 2. Materials and test procedure

The subject of the investigation is the construction steel 10HNAP, whose characteristics are given by the Polish Standard concerning low-alloyed and corrosion-resisting steel. 10HNAP is a weldable steel of general purpose and of increased resistance to atmospheric corrosion. Its chemical composition and mechanical properties are given in Table 1. Table 2 contains some parameters of the cyclic strain curve (10HNAP – cyclically stable material).

Table 1.

## Characteristic of 10HNAP steel

Steel	Chemical composition (wt. %)			Mechanical properties
10HNAP	0.14C	0.88Mn	0.31Si	$\sigma_y = 418 \text{ MPa}$ , $\sigma_u = 566 \text{ MPa}$ , $E = 2.15 \cdot 10^5 \text{ MPa}$ , $\nu = 0.29$
	0.066P	0.027S	0.73Cr	
	0.30Ni	0.345Cu		

Table 2.

## Cyclic properties of 10HNAP steel

Cyclic properties	
Cyclic strength coefficient, $K'$	832 MPa
Cyclic strain hardening exponent, $n'$	0.133
Fatigue strength coefficient, $\sigma'_f$	746 MPa
Fatigue strength exponent, $b$	-0.080
Fatigue ductility coefficient, $\epsilon'_f$	0.442
Fatigue ductility exponent, $c$	-0.601

The static properties of steel were determined in the laboratory of the Technical University of Opole. The cyclic strain curves for 10HNAP steel were obtained from the tests done at the Laboratoire de Mécanique et Physique des Matériaux ENSMA – CNRS Futuroscope – Chasseneuil, France. The tests were done on a fatigue stand INSTRON using the strain gages 5N. The cyclic strain curves were approximated with the Ramberg-Osgood relation:

$$\Delta \epsilon = \frac{\Delta \sigma}{E} + 2 \left( \frac{\Delta \sigma}{2K'} \right)^{\frac{1}{n'}} \quad (1)$$

The critical value of the integral for 10HNAP steel is  $J_{Ic} = 0.178 \text{ MPa}\cdot\text{m}$  [14], and the threshold integrals ranges are  $\Delta J_{th} = 1.35 \cdot 10^{-3} \text{ MPa}\cdot\text{m}$  for  $R = -1$  and  $\Delta J_{th} = 7.88 \cdot 10^{-4} \text{ MPa}\cdot\text{m}$  for  $R = -0.5$  and  $\Delta J_{th} = 3.84 \cdot 10^{-4} \text{ MPa}\cdot\text{m}$  for  $R = 0$  (calculated according to [15], assuming that  $\Delta J_{th} = (1 - \nu^2) \Delta K_{th}^2 / E$ ).

The tested specimens were cut of 10 mm thick plate in the rolling direction. Figure 1 shows the shape and the dimensions of the specimen. The specimen dimensions, length  $l$ , width  $b$  and thickness  $g$ , were  $250 \times 35 \times 8 \text{ mm}$ . In the centre, the specimens had round slots, 4 mm in diameter, with lateral incisions 1mm in length ( $2a_0 = 6 \text{ mm}$ ) and the rounding radius  $\rho = 0.125 \text{ mm}$ .

The notches in the specimens subjected to tension-compression were made by the electrospark method. The specimen surfaces were polished after grinding. The theoretical stress concentration factor in the specimen  $K_t = 8.87$ , was estimated with the use of the model [16]. The tests were

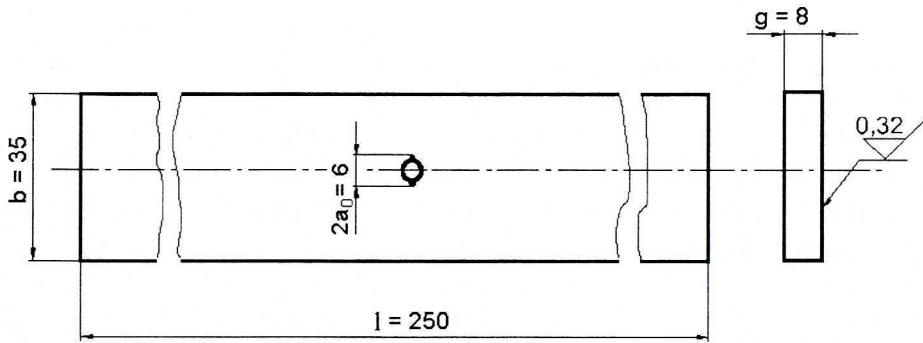


Fig. 1. Shape and dimensions of specimen for tests of fatigue crack extension

done on a (hydraulic machine produced by Werkstoffprüfmaschinen Leipzig) fatigue test stand SHM – 250 [11] under the loading frequency of 13 Hz.

The test stand SHM-250 makes it possible to carry out fatigue tests under uniaxial tension-compression with any loading mean value. The tests can be done under controlled force or deflection. The initial crack length in the notch was  $a = 0$ . In the tested specimens, the fatigue crack started propagating after some cycles in the notches. Thus, the specimen stiffness changed under invariable course of loading amplitude  $P_a$ .

The crack growth length was measured with an optical device including the digital micrometer and the microscopic telescope of 25-fold magnification. The applied digital micrometer, made by Mitutoyo Corporation, Japan, has got a certificate of calibration and its accuracy was 0.001 mm. The fatigue crack length was periodically measured after several thousand cycles, with an accuracy not less than 0.01 mm. At the same time, the number of loading cycles  $N$  was recorded. An MTS type extensometer was used in the tests, whose measuring basis is 10 mm. It is a model 632, 13F-20 produced by Systems Corporation Eden Prairie, USA. During the tests a hysteresis loop, strains and deflections were registered. The crack length increase on both sides of the specimens in relation to thickness was uniform.

Specimens were subjected to cyclic tension-compression at the constant amplitude of load  $P_a = 15$  kN. The stress ratio range was, respectively;  $R = \sigma_{\min} / \sigma_{\max} = -1, -0.5, 0$ . The mean force was  $P_m = (0, 5, 15)$  kN, respectively.

In order to describe the entire crack kinetics curve in an energy approach, the Forman et al. [17] formula is used, which refers to II and III crack growth stages (the stress criterion). The Klesnil and Lukas [18] equation, which describes I and II crack stages, was introduced into the formula. After combining these two equations, the whole crack curve was obtained in a

stress approach. The parameters  $\Delta K$  and  $K_{Ic}$  were replaced by the  $\Delta J$  integral range and  $J_{Ic}$ . Knowing that  $J = K^2/E$ , one introduced the relation  $(1 - R)^2 J_{Ic}$  resulting from analysis of linear crack mechanics equations. It substituted the expression with the stress ratio  $(1 - R) K_{Ic}$ .

The J-integral or its range  $\Delta J$  allows us to determine intensity of energy development for the case where a great plastic zone occurs in the crack tip area. For description of the curve of crack growth kinetics, the empirical formula was proposed [11]

$$\frac{da}{dN} = D \left[ \frac{\Delta J - \Delta J_{th}}{(1 - R)^2 J_{Ic} - J_{max}} \right]^p, \quad (2)$$

where  $\Delta J = J_{max} - J_{min}$ ,  $D$  and  $p$  characterize the material properties. The  $\Delta J$  integral range was calculated as the sum of elastic and plastic integrals from the equation (see Appendix)

$$\Delta J = \pi Y^2 \left[ (1 - \nu^2) \frac{\Delta \sigma^2}{E} + \frac{\Delta \sigma \Delta \epsilon_p}{\sqrt{n'}} \right] a, \quad (3)$$

Eq. (3) is determined in a straight-forward manner by computing only plastic strain energy density. Determination of  $\Delta J$  parameter in the presented empirical formula (2) constitutes an important, but on the other hand a difficult problem. The obtained test results allow us to formulate a model description of the crack kinetics curve in energy approach for 10HNP steel.

### 3. Experimental results and discussion

Graphs of the fatigue crack growth rates  $da/dN = f(\Delta J)$  for the steel tested under three stress ratios  $R$  are shown in Figure 2. It shows the results obtained from tests for  $\Delta J$  calculated from Eq. (3). Fig. 2 presents also approximation of the results by curve (2). This curve includes the threshold value range  $\Delta J_{th}$ , stress ratio  $R$  and the critical value of  $J_{Ic}$ . In the relation (2), the coefficients  $D$  and  $p$  determined during experiments can be treated as material constants. However, these constants actually depend not only on the kind of material but also on its other properties, for example on the stress ratio. For the relation (2) and 10HNP steel the constants are  $D = 3.30 \cdot 10^{-7}$  m/cycle and  $p = 0.65$ . The threshold integral ranges determined during experiments are close to the calculated ones [15] (relative error does not exceed 5%) and they are  $\Delta J_{th} = 1.41 \cdot 10^{-3}$  MPa·m ( $R = -1$ ),  $\Delta J_{th} = 8.11 \cdot 10^{-4}$  MPa·m ( $R = -0.5$ ) i  $\Delta J_{th} = 4.03 \cdot 10^{-4}$  MPa·m ( $R = 0$ ). A change of the stress ratio from  $R = -1$  to  $R = -0.5$  (Fig. 2) under the same loading amplitude  $P_a = 15$  kN and the integral range  $\Delta J = 2 \cdot 10^{-3}$  MPa·m causes two-fold increase in the fatigue crack growth rate. Fig. 2 it follows on that

there is a good agreement between the results obtained according to the proposed empirical formula (2) and the experimental results expressed in terms of  $\Delta J$  specified by Eq. (3). The maximum relative error of the test results amounts to 13% for correlation at the significance level  $\alpha = 0.05$ :  $r = 0.98$  for  $R = -1$ ,  $r = 0.99$  for  $R = -0.5$  and  $r = 0.99$  for  $R = 0$ . The coefficient  $D$  and the exponent  $p$  occurring in the relation (2) were determined by the least square method.

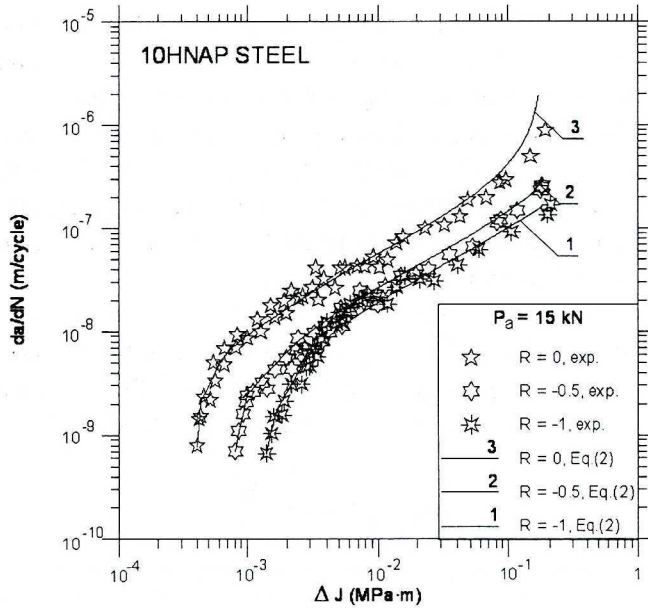


Fig. 2. Crack growth rates: comparison of experimental and predicted rates to relation (2) for 10HNAP steel

In the threshold value range, when short fatigue cracks appear, plasticity does not take place and it is possible to use linear-elastic fracture mechanics (applying the stress intensity factor range  $\Delta K$ ). As indicated in Fig. 2, an unstable behaviour occurs at high  $\Delta J$  values and it causes a rapid increase of crack growth rate just before total failure of the specimen (approaching the critical integral  $J_{Ic}$ ). There are two possible causes for such a behaviour. First, the increasing crack length during constant load testing causes the peak stress intensity to reach the value critical for the material, and an unstable behaviour is related to the early stages of brittle fracture [9]. This reason of the fatigue crack growth rate concerns brittle materials where stress is the dominating factor, and the test results concern mainly linear crack mechanics. The other reason for the increasing cracking causes diminishing of uncracked area of the specimen, with respect to the maximum loading causing total plastification of the material under limited loading. Then, application of coefficient  $K$  or

its range  $\Delta K$  for description of test results seems to be useless, because limitations of linear-elastic fracture mechanics are not valid. Elastic-plastic and plastic materials are subjected to large plastic deformations. The test results can be interpreted by the concept of a mean of  $\Delta J$ -integral range, which includes both stresses and strains in the crack tip.

### 3.1. Relationship between $\Delta K$ and $\Delta J$

While calculating  $\Delta J$ -integral range, we can find that there is a functional relation between the loading range, the elastic-plastic strain range, the crack opening and the crack length. Large values of correlation coefficients show that all these factors are approximately included. Above a certain value of  $\Delta J$ -integral range, the crack growth rate increases rapidly without further increase of loading. This behaviour is connected with an unstable crack growth rate at the final stage of specimen life. In this period, also a loading decrease is observed as plastification increases.

Application of the  $\Delta J$  parameter is reasonable in the case of elastic-plastic materials and those with a distinct yield point. In order to show that application of  $\Delta J$ -integral range is correct, we analysed the correlation between the parameters  $\Delta K$  and  $\Delta J$ . The following relation was used

$$\Delta J^* = (1 - \nu^2) \frac{\Delta K^2}{E}, \quad (4)$$

where  $\Delta K = K_{\max} - K_{\min} = Y\Delta\sigma\sqrt{\pi(a+a_0)}$  and  $\Delta\sigma = \sigma_{\max} - \sigma_{\min}$  ( $\Delta\sigma = 2\sigma$  for  $R = -1$ ).

Fig. 3 shows the relation between the parameters  $\Delta J^*$  and  $\Delta J$  for three stress ratios  $R$ . One can see a good linear relation (in a double logarithmic system) between these two parameters in the case of the fatigue crack growth rate for the tested steel.

In 10HNAP steel, this takes place for  $\Delta J < 1 \cdot 10^{-2}$  MPa-m (Fig. 3). It means that in these tests ranges under controlled loading, the parameter  $\Delta J$  plays a similar role like  $\Delta K$  up to the moment when plastic strain occurs. When plastic strains increase it has been found that the difference between  $\Delta J^*$  and  $\Delta J$  increases. This difference results from the fact that the parameter  $\Delta J^*$  does not account for plastic strains. At the final stage of specimen lives, when  $\Delta J$ -integral range approaches the critical value of  $J_{Ic}$ , the crack growth rate increases rapidly (Fig. 3,  $R = 0$ ) and leads to material failure.

For example, in Fig. 4 ( $R = -0.5$ ) fatigue crack length  $a$  versus the number of cycles  $N$  and  $\Delta J$ -integral range versus the number of cycles  $N$  are shown in a linear system. In this figure, we can observe fatigue crack growth since the beginning of the propagation until the specimen failure. In Fig. 4,

the graph  $\Delta J$  versus  $N$  also shows that  $\Delta J$ -integral range increases with the number of cycles until reaching 440000 cycles, then the graph stabilises (the value becomes almost constant).

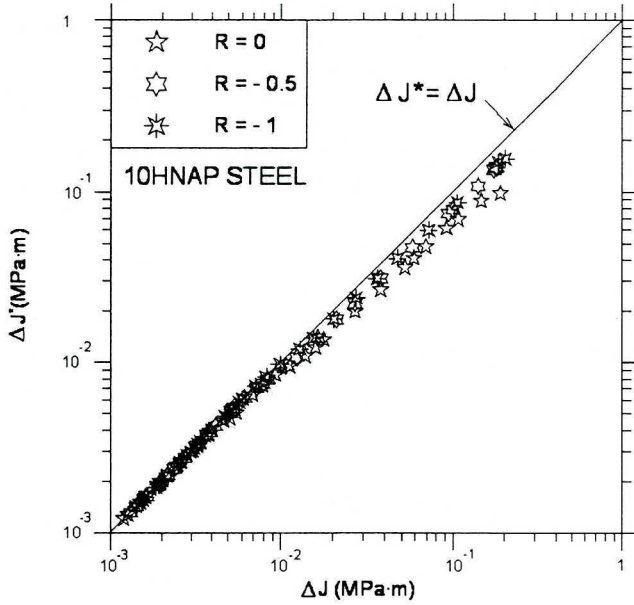


Fig. 3. The relationship between  $\Delta J^*$  and  $\Delta J$  for 10HNAP steel

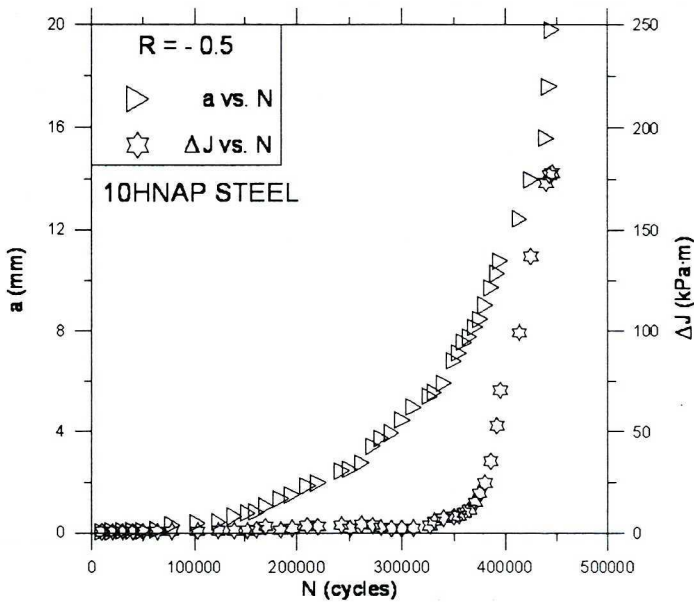


Fig. 4. Variation of crack length in cyclic loading process and  $\Delta J$  for  $R = -0.5$

### 3.2. FEM analyses

The  $\Delta J$ -integral range, i.e. values of  $J_{\max}$  and  $J_{\min}$  were numerically determined with the finite element method (FEM). For this purpose, the program FRANC2D was applied. It allows calculating energy dissipated during the fatigue crack growth in the elastic-plastic material. A specimen model was built and divided into finite elements with the use of CASCA graphic processor, which was integrated with program FRANC2D. After making a specimen contour, the lengths were distinguished and closed areas were defined. Each of these areas was covered with a net of finite elements. The net is constructed by the program automatically. Figure 5 shows the division of the area around the crack into finite elements. In the model, six-nodal triangular elements were applied; the triangles were of different dimensions. The size and shape of finite elements depend on the division of lengths closing each area. The highest density of the net is found in the area of fatigue crack growth (Fig. 5). Next one of the specimen ends is restrained (taking away the degrees of freedom off the specimen nodes) and it is fixed in the direction of  $x$  or  $y$  axis or in both directions simultaneously. In order to perform numerical calculations it is necessary to introduce material data, such as: yield stress, Young's modulus, Poisson's ratio, specimen thickness and to load the cyclic strain curve, described by the Ramberg-Osgood relation (1) into the program FRANC2D. Once these values are introduced, the loading should be defined. The calculations are carried out after a force is applied. Program FRANC2D does calculations in the range of linear-elastic and elastic-plastic fracture mechanics. The calculations are done in the incremental way for flat notched specimen (Fig. 1), and in the elastic-plastic range the Newton-Raphson iterative method is applied.

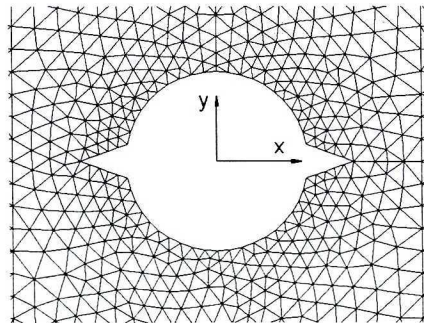


Fig. 5. Division of the notch region into finite elements mesh

In the notches, the fatigue crack (as it was shown by observations) was initiated, which propagates along the cross section of the specimen. For

calculations, the same loading values as those used in experiments were assumed.

Test results associated with  $\Delta J$  specified by (Eq. 3) were compared with the finite element calculation results, see Fig. 6. It can be noticed that the experimental results are consistent with those obtained with FEM in the threshold range and for linear crack growth. Differences between the presented results (Fig. 6) appear when the increase in plasticity occurs ( $\Delta J = 9.7 \cdot 10^{-3}$  MPa·m). Higher values of  $\Delta J$  at the same level of fatigue crack growth rate occur for the results obtained from Eq. (3). The biggest differences between the test results can be found at the end of specimen life. As the stress ratio  $R$  rises from  $-1$  to  $0$ , we observe an increase in the  $\Delta J$ -integral range described by Eq. (3) in relation to FEM. The greatest differences in the test results exist when the stress ratio  $R = 0$  approaches the critical value of the integral  $J_{Ic}$ . The relative error between the results does not exceed 20%.

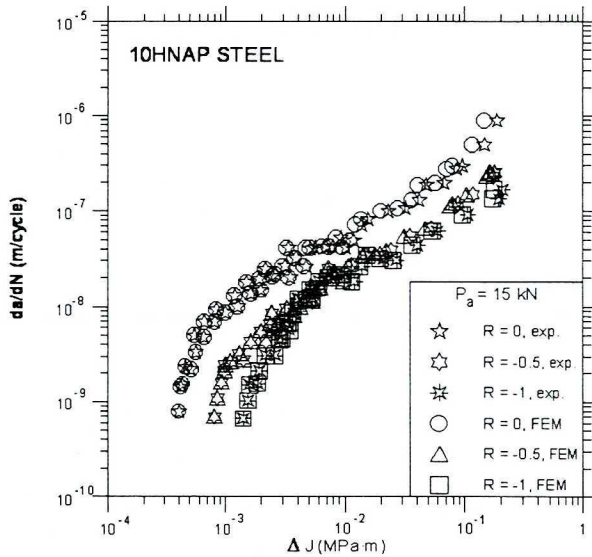


Fig. 6. Comparison of the experimental results based on Eq. (3) with FEM calculation results

### 4. Conclusions

The presented results of the fatigue crack growth in steel subjected to cyclic tension-compression loading under three stress ratios allow us to formulate the following conclusions:

1. The applied empirical formula (2) including the  $\Delta J$ -integral range describes well the test results of the fatigue crack growth kinetics curve in the steel tested.

2. It has been shown that the application of the  $\Delta J$  parameter for different  $R$  is better for description of the crack growth rate in the considered steel than  $\Delta K$ .
3. It has been shown that there are differences in description of the  $\Delta J$ -integral range between the proposed Eq. (3) and FEM. The relative error does not exceed 20%.
4. It has been proved that the change of the stress ratio from  $R = -1$  to  $R = 0$  increases the fatigue crack growth rate.

This work was supported by the Commission of the European Communities under the FP5, GROWTH Programme, contract No. G1MA-CT-2002-04058 (CESTI).

## APPENDIX

### Development of equation

The J-integral of a cracked specimen can be expressed as follows, [19]:

$$J = 2\pi Y^2 a \int_0^{\varepsilon} \sigma d\varepsilon, \quad (A1)$$

where  $\int_0^{\varepsilon} \sigma d\varepsilon$  – strain energy density.

As mentioned previously, in the case of cyclic loading the total  $\Delta J$ -integral range can be divided into elastic and plastic components:

$$\Delta J = \Delta J_e + \Delta J_p = 2\pi Y^2 \left( \int_0^{\Delta \varepsilon_e} \sigma d\varepsilon_e + \int_0^{\Delta \varepsilon_p} \sigma d\varepsilon_p \right) a, \quad (A2)$$

where  $Y = \sqrt{\frac{b}{\pi a} \operatorname{tg} \frac{\pi a}{b}}$ ,  $a$  – crack length,  $b$  – width specimen.

Fig. A1 shows cyclic stresses and strains based on the hysteresis loop.

In Eq. (A2), the elastic part of  $\Delta J_e$ , after integration for plane strain state (It was found that there was an influence of the specimen thickness, and the relative error of the compared methods was above 10%.) is:

$$\Delta J_e = 2\pi Y^2 (1 - \nu^2) \left( \frac{\Delta \sigma^2}{2E} \right) a = \pi Y^2 (1 - \nu^2) \left( \frac{\Delta \sigma^2}{E} \right) a. \quad (A3)$$

The plastic part can be written as

$$\Delta J_p = 2\pi Y^2 \left[ \frac{f(n')}{1+n'} \Delta\sigma \Delta\varepsilon_p \right] a. \tag{A4}$$

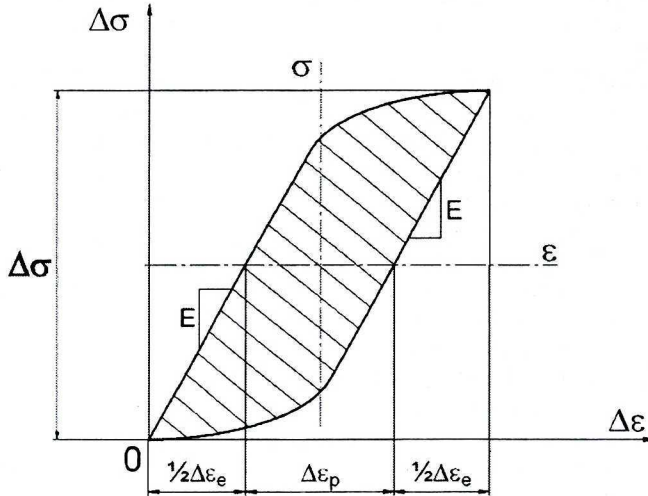


Fig. A1. The cyclic stress-strain hysteresis loop

Using the Dowling proposal [20], we can determine function  $f(n')$  for flat specimens with central cracks (Fig. 1) for slightly hardening materials or cyclically weakening as  $f(n') = (1+n')(1/2\sqrt{n'})$  and after introduction to (A4) we obtain

$$\Delta J_p = \pi Y^2 \left( \frac{\Delta\sigma \Delta\varepsilon_p}{\sqrt{n'}} \right) a. \tag{A5}$$

Function  $f(n')$  is right assuming that the initial crack is considerably smaller than the specimen width.

After substituting Eqs. (A3) and (A5) to (A2) we obtain the total  $\Delta J$ -integral range as

$$\Delta J = \pi Y^2 \left[ \left(1 - \nu^2\right) \frac{\Delta\sigma^2}{E} + \frac{\Delta\sigma \Delta\varepsilon_p}{\sqrt{n'}} \right] a. \tag{A6}$$

## REFERENCES

- [1] Priddle E. K.: Some equations describing the constant amplitude fatigue crack propagation characteristics of a mild steel. Berkeley Nuclear Laboratories, 1972, RD/B/N 2390.
- [2] Jarema S. J. and Mikitisin S. I.: Analiticeskoje opisanie diagramy ustalostnogo razrusenia materialov. Fiziko-chemiceskaja Mehanika Materia3ov, Vol. 6, 1975, pp. 47÷54 (in Russian).
- [3] McEvily A. J.: On closure in fatigue crack growth. ASTM STP 982, 1988, pp. 35÷43.
- [4] Toth L., Krasovsky A. J.: Material characterization required for reliability assesment of cyclically loaded engineering structures. Ed. R.A. Smith, Kluwer Academic Publisher, 1997, pp. 225÷272.
- [5] Gasiak G., Pawliczek R., Rozumek D.: Life of constructional materials under cyclic loading including the mean loading values. Technical University of Opole, 2002, p. 312 (in Polish).
- [6] Kocanda S.: Fatigue failure of metals. WNT, Warsaw, 1985, pp. 441.
- [7] Rice J. R.: A path independent integral and the approximate analysis of strain concentration by notches and cracks. Journal of Applied Mechanics, Vol. 35, 1968, pp. 379÷386.
- [8] Begley J. A. and Landes J. D.: The J-integral as a fracture criterion. Fracture Toughness, ASTM STP 514, 1971, pp. 1÷20.
- [9] Dowling N. E. and Begley J. A.: Fatigue crack growth during gross plasticity and the J-integral. In Mechanics of Crack Growth, ASTM STP 590, 1976, pp. 82÷103.
- [10] Gasiak G., Rozumek D.:  $\Delta J$ -integral range estimation for fatigue crack growth rate description. Int. J. of Fatigue, Vol. 26, 2004, pp. 135÷140.
- [11] Rozumek D.: Kinetic crack growth curve in energetic approach. WNT, 2003, pp. 435÷442 (in Polish).
- [12] Lu Y. L. and Kobayashi H.: An experimental parameter  $J_{max}$  in elastic-plastic fatigue crack growth. Fatigue & Fracture of Eng. Mater. & Struct., Vol. 19, 1996, pp. 1081÷1091.
- [13] Tanaka K.: The cyclic J-integral as a criterion for fatigue crack growth. Int. J. Fracture, Vol. 22, 1983, pp. 91÷104.
- [14] ASTM E813-89. Standard test method for  $J_{Ic}$ , a measure of fracture toughness. American Society for Testing and Materials, Philadelphia, 1989.
- [15] Vosikovskiy O.: The effect of stress ratio on fatigue crack growth rates in steel. Eng. Fracture Mechanics, 1979.
- [16] Thum A., Petersen C., Swenson O.: Verformung, Spannung und Kerbwirkung. Dusseldorf, VDI, 1960.
- [17] Forman R. G., Kearney V. E., Engle R. M.: Numerical analysis of crack propagation in cyclic-loaded structures. Journal of Basic Eng., 1967, pp. 459÷464.
- [18] Klesnil, M., Lukas, P.: Influence of strength and stress history on growth and stabilisation of fatigue cracks. Eng. Fracture Mechanics, Vol. 4, 1972, pp. 77÷92.
- [19] Cai Qi-Gong.: Analysis of elastic-plastic fracture mechanics of the cyclic strain. New Metals, China, Vol. 1, 1976, pp. 102.
- [20] Dowling N. E.: Crack growth during low-cycle fatigue of smooth axial specimens. In: Cyclic stress-strain and plastic deformation aspects of fatigue crack growth, ASTM STP 637, 1977, pp. 97÷121.

**Całka J w opisie sprężysto-plastycznej krzywej kinetyki wzrostu pęknięcia****Streszczenie**

W pracy zaprezentowano krzywą kinetyki wzrostu pęknięcia zmęczeniowego dla stali 10HNAP, którą zweryfikowano doświadczalnie. Przedstawiono podejście energetyczne oparte na całce  $\Delta J$ .

Badania prowadzono na próbkach płaskich z karbem przy rozciąganiu-ściskaniu dla trzech wartości współczynnika asymetrii cyklu  $R$ . Całkę  $J$  obliczano analitycznie i metodą numeryczną z zastosowaniem metody elementów skończonych (MES). Zaproponowano związek do opisu całej krzywej kinetyki wzrostu pęknięcia z wykorzystaniem całki  $J$ . Wykazano, że przy stałej amplitudzie obciążenia rozciągającego-ściskającego i zmianie współczynnika asymetrii cyklu z  $R = -1$  na  $R = 0$  wzrasta prędkość pęknięcia zmęczeniowego. Zaproponowany w pracy związek do opisu krzywej kinetyki wzrostu pęknięcia daje wyniki zbieżne z doświadczalnymi i uzyskanymi przy użyciu MES.